Progress In Electromagnetics Research B, Vol. 26, 401–423, 2010

THE DIPOLE IMPEDANCE OF AN APERTURE

R. Stoneback

W. B. Hanson Center for Space Sciences
University of Texas at Dallas, USA

Abstract—The dipole impedance of an aperture in a plane conductor is obtained by modifying the general network formulation of electromagnetic apertures presented by Mautz and Harrington. The derived dipole impedances are combined in parallel to form an effective circuit description of low frequency aperture diffraction. Power transmitted into the aperture by an incident wave is determined by incorporating standard techniques for the transfer of wave power at an impedance mismatch. This transmitted power is divided into forward and backward scattered fields based upon the behavior of image currents surrounding the aperture, leading to a peak in forward scattered power above unity, consistent with known aperture behavior. The presented aperture circuit maintains an excellent correspondence with measurements of radiated power for an aperture excited by high energy electrons and with the numerically calculated impedance of a circular aperture using the finite element method.

1. INTRODUCTION

Previous work applies the method of moments [1] to the electromagnetic boundary conditions in an aperture [2] to construct a general network formalism capable of solving aperture coupling problems [3–8]. The method has been used to study apertures in thick conductors [9], apertures surrounded by dissimilar media [10], the coupling of an aperture with a wire [11] or a capacitor [4], as well as a cavity backed slit [12].

In the long wavelength limit, this framework may also be used along with known electric and magnetic aperture dipole

Received 24 June 2010, Accepted 28 October 2010, Scheduled 5 November 2010
Corresponding author: Russell Stoneback (rstoneba@utdallas.edu).

moments [13, 14] to calculate the admittance of an aperture. However, the equivalent impedances obtained in [4, 5, 7] are not consistent with the Finite Element Method (FEM) results presented here. The FEM analysis has been verified by comparison to [15] and [16], thus this disparity is considered significant.

Modifications to [5] presented here are used to obtain a simple analytic description of the aperture dipole impedance. The derived impedance is consistent with FEM results and a calculation of radiated power using the presented aperture model closely follows measurements of a circular aperture excited by a high energy electron beam [17], supporting the derived expressions.

One source of error in previous attempts [5] is the symmetric (dot) product definition which introduces units of area. Combined with normalizations chosen based upon this symmetric product, the resulting aperture impedances are incorrect by a factor of aperture area. The dot product also leads to an aperture electric dipole impedance calculation that utilizes an equivalence between electric and magnetic dipoles [5]. By adopting a modified symmetric product here, the ratio of currents that create the equivalent electric/magnetic dipoles are used instead. This change results in a new term in the aperture impedance that is equivalent to the effective thickness of an infinitely thin acoustic aperture [18, 19].

The impedance of an aperture previously [5, 10] depended upon the materials on both sides of an aperture. However, numerical results presented here demonstrate that the aperture impedance is only dependent upon the region not containing the incident wave source. In addition, the relationships between effective moments on either side of the aperture are modified from the previous parallel distribution [5]. It is shown that the magnetic dipoles act in series while the electric dipole has a parallel distribution.

The impedance of the magnetic and electric dipoles were previously treated separately when calculating aperture fields. Here, the impedances are combined together as if part of a single circuit. The interaction of these electric and magnetic dipole impedances leads to a radiated power that goes to zero in the high frequency limit. Previous dipole solutions [4, 5, 7, 13, 14] along with more recent attempts using a different methodology [20] lead to infinite radiated power in the high frequency limit.

By obtaining the impedance of an aperture, the power transmitted from a system through an aperture can be calculated incorporating standard relations for waves at the interface between two media. Power transmitted into the aperture impedance is divided into forward and scattered fields by the use of image currents. In the low frequency

limit, power is shared equally between the forward and backward scattered fields. As wavelengths approach the size of the aperture, the power radiated by the back scattered image field switches direction, contributing to the forward scattered field. In this regime, the aperture radiates more power than is directly incident upon it, consistent with previous numerical solutions [15] and measurements of a single aperture in a metal [17]. The increase in radiated power can be enhanced with an array of apertures due to plasmon (surface wave) resonances [21, 22].

For clarity, the derivation of the modified network formulation is presented in Section 2. This framework is then applied to the specific case of the dipole response of a circular aperture in a plane conductor in Section 3. The power transmitted into and radiated by the aperture is constructed in Section 4 and compared to numerical (Section 5) and experimental [17] results in Section 6.

2. NETWORK FORMULATION

Consider a plane perfect conductor with an aperture in Fig. 1. Region 1 to the left of the conductor is characterized by μ_1, ϵ_1, region 2 to the right is characterized by μ_2, ϵ_2 and there are incident waves in both regions. Bethe [13] found that if the aperture is small compared to the incident wavelength a solution may be obtained by replacing the aperture with a conductor containing magnetic currents. Replacing the aperture with a conductor removes the mixed boundary conditions present in the original formulation while the magnetic currents recreate the aperture fields. A linear superposition of the incident wave reflecting from the perfect conductor and the fields created by the aperture equivalent magnetic currents recreate the fields in the original problem. In this low frequency regime, the diffracted field can be approximated using a combination of electric and magnetic dipoles in place of the aperture.

To maintain equivalence between the introduced magnetic currents and the aperture electric field, the magnetic current density $\mathbf{M}$ is constrained by

$$\mathbf{M} = \mathbf{E} \times \hat{n}_{12} \tag{1}$$

where $\mathbf{E}$ is the electric field in the aperture in the original problem and $\hat{n}_{12}$ is a unit vector normal to the conductor pointing from region 1 to region 2.

Building upon the framework detailed by Mautz and Harrington [5], suppose that the electric and magnetic fields in region 1 may

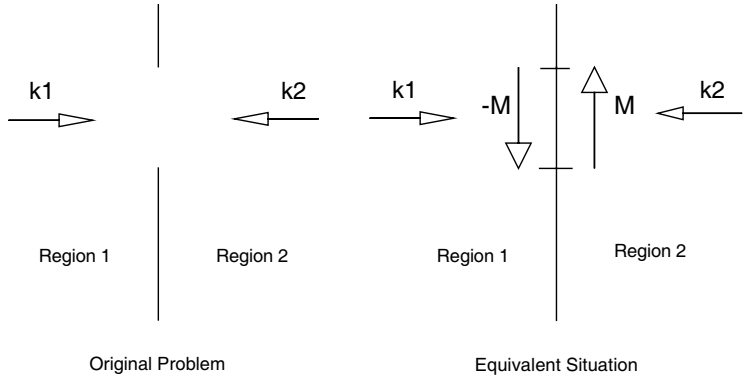

Figure 1. Geometry of original problem and an equivalent situation.

be written

$$\mathbf{E}_1 = \mathbf{E}_1(-\mathbf{M}) + \mathbf{E}_{1s} \tag{2}$$

$$\mathbf{H}_1 = \mathbf{H}_1(-\mathbf{M}) + \mathbf{H}_{1s} \tag{3}$$

where $\mathbf{E}_1$ is the total field in region 1 in the original problem, $\mathbf{E}_{1s}$ is the field produced by the incident plane wave and its reflection from the plane conductor with shorted aperture (aperture replaced with conductor) and $\mathbf{E}_1(-\mathbf{M})$ is the field produced by the magnetic current in place of the aperture in region 1. Similar relations are obtained for region 2 where $-\mathbf{M} \rightarrow \mathbf{M}$ for continuity of the tangential electric field [7].

The continuity of the tangential component of the magnetic field across the aperture requires

$$-\mathbf{H}_1^{\tan}(\mathbf{M}) - \mathbf{H}_2^{\tan}(\mathbf{M}) = -(\mathbf{H}_{1s}^{\tan} - \mathbf{H}_{2s}^{\tan}) \tag{4}$$

and continuity of the normal component of the displacement field requires

$$\epsilon_1 \mathbf{E}_1^{nrm}(\mathbf{M}) + \epsilon_2 \mathbf{E}_2^{nrm}(\mathbf{M}) = \epsilon_1 \mathbf{E}_{1s}^{nrm} - \epsilon_2 \mathbf{E}_{2s}^{nrm}. \tag{5}$$

Given that the aperture may be considered as an electric and magnetic dipole in the low frequency limit ($ka << 1$) [13], where a is the aperture radius, the aperture equivalent magnetic current $\mathbf{M}$ may be separated into three components [5]

$$\mathbf{M} = V_e \hat{M}_e + V_{h\beta} \hat{M}_{h\beta} + V_{h\gamma} \hat{M}_{h\gamma} \tag{6}$$

where $\hat{M}_e, \hat{M}_{h\beta}$ and $\hat{M}_{h\gamma}$ are current distributions over the aperture (dimensionless) that lead to electric and magnetic dipoles in the far

field, approximated here using constant unit vectors, $\hat{M}_{h\beta} = \hat{\beta}, \hat{M}_{h\gamma} = \hat{\gamma}$ and $\hat{M}_e = \hat{\theta}$. The vectors $\hat{\beta}$, $\hat{\gamma}$ are orthonormal and in the plane of the aperture. V_e is the magnitude of the electric dipole current while $V_{h\beta}, V_{h\gamma}$ account for the pair of magnetic dipoles in the plane of the aperture. The combination of currents for the magnetic dipole accounts for the orientation of the incident magnetic field with respect to the aperture. In general it is presumed that the choice of $\hat{M}_{h\beta}, \hat{M}_{h\gamma}$ diagonalize the aperture polarizability tensor [5].

Substituting the magnetic current expansion (6) into the magnetic field continuity equation (4), the contribution from each current can be isolated using an average symmetric product

$$< A, B >= \frac{\int \mathbf{A} \cdot \mathbf{B}\, dS}{S} \tag{7}$$

and the orthogonality of the basis functions. This symmetric product differs from [5] by normalizing the product by the aperture area. This is necessary to maintain the units of quantities in the symmetric product.

The contribution from aperture currents along $\hat{M}_{h\beta}$ is

$$-V_{h\beta} < \mathbf{H}_1^{\tan}(\hat{M}_{h\beta}) + \mathbf{H}_2^{\tan}(\hat{M}_{h\beta}), \hat{M}_{h\beta} >= - < \mathbf{H}_{1s}^{\tan} - \mathbf{H}_{2s}^{\tan}, \hat{M}_{h\beta} > \tag{8}$$

where the linearity of the magnetic field allows

$$H_1^{\tan}(V_{h\beta}\hat{M}_{h\beta}) = V_{h\beta} H_1^{\tan}(\hat{M}_{h\beta}). \tag{9}$$

Since $V_{h\beta}$ carries units V/m which $H_1^{\tan}(\hat{M}_{h\beta})$ now lacks,

$$[Y_1 + Y_2]_{h\beta} = - < \mathbf{H}_1^{\tan}(\hat{M}_{h\beta}) + \mathbf{H}_2^{\tan}(\hat{M}_{h\beta}), \hat{M}_{h\beta} > \tag{10}$$

is an averaged admittance of the aperture to magnetic fields. Furthermore,

$$I_{h\beta} = - < \mathbf{H}_{1s}^{\tan} - \mathbf{H}_{2s}^{\tan}, \hat{M}_{h\beta} > \tag{11}$$

is the averaged tangential magnetic field along $\hat{M}_{h\beta}$ exciting the aperture, interpreted to be an effective input current. Substitution into (8) yields a generalized Ohm's law relating the averaged magnetic current representing the aperture field ($V_{h\beta}$) to the averaged effective current representing the input magnetic field ($I_{h\beta}$)

$$V_{h\beta}[Y_1 + Y_2]_{h\beta} = I_{h\beta}. \tag{12}$$

A similar network relation can be found along γ by replacing $\beta \to \gamma$.

Though (10)–(12) visually appear the same as found in [7], the previous admittance and current vectors contain additional units of area. Further, the magnetic currents were treated as point currents at the aperture origin while here they are treated as averaged currents over the aperture.

Following the same procedure for the electric field, the magnetic current expansion (6) is substituted into the continuity equation for displacement fields (5). Since the magnetic current $\hat{M}_e$ is orthogonal to the electric field it produces, an equivalent electrical current is used instead [5]. Consider that the electric dipole field created by a magnetic current loop $\mathbf{K}$ surrounding area S will also be produced by an electric current I over some length l normal to S [23, pg. 135] when

$$Il = -j\omega\epsilon_i KS. \tag{13}$$

Strictly, the equivalence of the fields produced by these currents is only maintained when l is infinitesimally short and K, I are infinitesimally thin. However, the restrictions may be relaxed if equivalence is only required for fields far from the currents. Deviating from [5] and supposing the aperture dipoles have a finite length yields an admittance

$$\frac{I}{K} = -j\omega\epsilon_i \frac{S}{l_e} \tag{14}$$

that relates a magnetic current to an equivalent electrical current in the aperture. Further, for long wavelengths, the infinitesimal electric and magnetic current elements may be replaced by electric ($\mathbf{J}$) and magnetic ($\mathbf{M}$) current densities over the aperture,

$$\frac{J}{M} = -j\omega\epsilon_i b \tag{15}$$

which may be used to convert incident electric fields to equivalent aperture input currents, where

$$b = \frac{S}{l_e} \tag{16}$$

is interpreted as an effective minimum thickness of the aperture, described in more detail below. Using (15), the electrical current equivalent to the aperture magnetic current $V_e\hat{M}_e$ is

$$\vec{J_e} = -j\omega\epsilon_o b V_e \hat{z} \tag{17}$$

which differs from previous results [5] by the factor b.

The magnetic dipole length l_n is obtained by integrating the path length of the magnetic currents on both sides of the aperture,

$$l_n = 2\int\int \hat{M}_n \cdot d\hat{l}'_n \; d\theta \tag{18}$$

where $\theta = 0$ is perpendicular to $\hat{M}_n$, for $n = \hat{\beta}, \hat{\gamma}$ and $d\hat{l}'_n$ is a differential length element along the current. Considering a circular aperture and using the approximation that the basis functions are unit vectors in

the aperture, $l_n = 8a$, while a rectangular aperture longer (l) than it is wide (w) has $l_n \approx 4w$. An aperture wider than long has $l_n \approx 2\pi w$ while a square aperture with length l has $l_n = \pi l$.

For the electric dipole length, the equivalent magnetic current is a loop current [5] and is not suitable for (18). However, it is known [24] that the electric aperture polarizability (α_e) is determined by a parallel combination of magnetic polarizabilities ($\alpha_{m\beta},\ \alpha_{m\gamma}$) along $\hat{M}_\beta,\ \hat{M}_\gamma$

$$\frac{1}{\alpha_e} = \frac{1}{\alpha_{m\beta}} + \frac{1}{\alpha_{m\gamma}}. \tag{19}$$

This relationship suggests that the electric dipole is the result of a parallel combination of magnetic dipoles. Thus, the electric dipole length l_e might be determined similarly.

Consider electric dipoles in the plane of the aperture by substituting $\hat{J}_n$ for $\hat{M}_n$ in (18). Since these electric dipoles are in the aperture plane, no power is detected in the far field. Rotating these electric dipole currents out of the aperture plane leads to radiated electric dipole power with characteristics of two dipole lengths, l_β and l_γ. For long wavelengths, this field is equivalent to a purely normal aperture electric dipole with a single characteristic length, l_e. Given this equivalence and the parallel distribution of polarizability (19), the effective electric dipole length is presumed to be a parallel combination of the two possible magnetic current lengths

$$\frac{1}{l_e} = \frac{1}{l_\beta} + \frac{1}{l_\gamma}. \tag{20}$$

For a circular aperture, $l_e = 4a$ and $b = \pi a/4$, the same effective thickness as an infinitely thin acoustic circular aperture radiating into a half space [18]. This result motivates the interpretation of b as a minimum effective thickness of an aperture for electromagnetic fields.

Applying the method of moments to the electric field including (17) yields

$$V_e[Y_1 + Y_2]_e = I_e \tag{21}$$

where

$$[Y_1 + Y_2]_e = < \frac{\epsilon_1}{\epsilon_o}\mathbf{E}_1^{nrm}(\hat{M}_e) + \frac{\epsilon_2}{\epsilon_o}\mathbf{E}_2^{nrm}(\hat{M}_e), -j\omega\epsilon_o b\hat{z} > \tag{22}$$

is the averaged admittance of the aperture for electric fields,

$$I_e = < \frac{\epsilon_1}{\epsilon_o}\mathbf{E}_{1s}^{nrm} - \frac{\epsilon_1}{\epsilon_o}\mathbf{E}_{2s}^{nrm}, -j\omega\epsilon_o b\hat{z} > \tag{23}$$

is the equivalent input current density for the source electric field and V_e is the magnitude of the aperture equivalent magnetic current density. The admittance and input current presented differ from [5] by the factor b and by dimensions of meters.

3. APERTURE DIPOLE IMPEDANCES

The dipole impedance of an aperture can be determined using the generalized Ohm's law relations obtained in the previous section and the aperture dipole moments [13]. The input currents are calculated from the incident fields exciting the aperture and the aperture equivalent magnetic current magnitudes are calculated using the known aperture dipole moments. The general structure of the impedance derivation follows [5], though differences exist and are noted.

For low frequencies, the basis functions have been chosen to be constant directions, $\hat{M}_{h\beta} = \hat{\beta}, \hat{M}_{h\gamma} = \hat{\gamma}$ and $\hat{J}_e \propto \hat{z}$ [5]. In this regime, the input currents reduce to

$$I_{h\beta} = -|\mathbf{H}_{1s}^{\tan} - \mathbf{H}_{2s}^{\tan}| \cos\theta \tag{24}$$

$$I_{h\gamma} = -|\mathbf{H}_{1s}^{\tan} - \mathbf{H}_{2s}^{\tan}| \sin\theta \tag{25}$$

$$I_e = -j\omega b(\epsilon_1 E_{1s}^{nrm} - \epsilon_2 E_{2s}^{nrm}) \tag{26}$$

where θ is the angle between $\hat{\beta}$ and $\mathbf{H}_{1s}^{\tan} - \mathbf{H}_{2s}^{\tan}$. The total effective current exciting the magnetic dipole is

$$I_h = \sqrt{I_{h\beta}^2 + I_{h\gamma}^2} = |\mathbf{H}_{1s}^{\tan} - \mathbf{H}_{2s}^{\tan}|. \tag{27}$$

Given the continuity of fields within the aperture, the aperture impedance must be the same in both regions 1 and 2. However, the impedances listed in [5, Eqs. (33)–(34)] vary across the aperture. To accurately reflect all of the fields in an aperture when determining the impedance, the half space dipole moments for each side of the aperture are combined rather than treated separately as in [5]. The half space dipoles radiating into region 2 [25] are

$$\mathbf{p}_{e2} = \frac{\epsilon_2}{\epsilon_1 + \epsilon_2} \alpha_e (\epsilon_1 E_{1s}^{nrm} - \epsilon_2 E_{2s}^{nrm}) \hat{n}_{12} \tag{28}$$

$$\mathbf{p}_{m2} = \frac{-\mu_1}{\mu_1 + \mu_2} (\alpha_{m\beta} \cos\theta \hat{\beta} + \alpha_{m\gamma} \sin\theta \hat{\gamma}) I_h \tag{29}$$

and the dipoles for region 1 are

$$\mathbf{p}_{e1} = \frac{-\epsilon_1}{\epsilon_1 + \epsilon_2} \alpha_e (\epsilon_1 E_{1s}^{nrm} - \epsilon_2 E_{2s}^{nrm}) \hat{n}_{12} \tag{30}$$

$$\mathbf{p}_{m1} = \frac{\mu_2}{\mu_1 + \mu_2} (\alpha_{m\beta} \cos\theta \hat{\beta} + \alpha_{m\gamma} \sin\theta \hat{\gamma}) I_h. \tag{31}$$

Since the moments in each region have opposite orientations, the difference between moments is used to determine the aperture impedance. For a source in region 1, radiating through the aperture

into region 2, the combined moments are

$$\mathbf{p}_e = \mathbf{p}_{e2} - \mathbf{p}_{e1} = \alpha_e(\epsilon_1 E_{1s}^{nrm} - \epsilon_2 E_{2s}^{nrm})\hat{n}_{12} \tag{32}$$

$$\mathbf{p}_m = \mathbf{p}_{m2} - \mathbf{p}_{m1} = -(\alpha_{m\beta}\cos\theta\hat{\beta} + \alpha_{m\gamma}\sin\theta\hat{\gamma})I_h \tag{33}$$

with equivalent dipole currents [5]

$$\mathbf{I}l = j\omega\mathbf{p}_e \tag{34}$$

$$\mathbf{K}l = j\omega\mu_2\mathbf{p}_m. \tag{35}$$

The fictional magnetic currents ($\mathbf{M}$) in the aperture will produce the same fields far from the aperture as the dipole currents (34), (35) if $\int \mathbf{K}d^3r = \int \mathbf{M}d^3r$ within the aperture, or

$$\mathbf{M} = \frac{\mathbf{K}l}{S}. \tag{36}$$

The integral of the loop current $\mathbf{K}$ yields a product with the dipole length, while the integral of the magnetic current density $\mathbf{M}$ distributed over the aperture yields a product with the aperture area.

Substitute (35) and the magnetic current expansion (6) into (36) to obtain $V_{h\beta}$. Using the generalized Ohm's Law (12) and the input current due to the incident field (24), the total imaginary admittance along $\hat{\beta}$ is

$$\mathrm{Im}[Y_1 + Y_2]_h^{\beta} = \frac{S}{j\omega\mu_2\alpha_{m\beta}} \tag{37}$$

with a similar relation along $\hat{\gamma}$.

For the real admittance, the power radiated by a magnetic dipole current near a conductor into region 2 with wave impedance Z_2 [23]

$$P = \frac{k_2^2|\mathbf{K}l|^2}{6\pi Z_2} \tag{38}$$

is normalized by the aperture area and (36) is used to replace the normalized dipole current with $\mathbf{M} = V_{hi}\hat{M}_i$,

$$\frac{P}{S} = \frac{Sk_2^2}{6\pi Z_2}|V_{hi}|^2 = \frac{1}{2}|V_{hi}|^2 Y. \tag{39}$$

The radiated power density is used rather than the total radiated power as in [5] since the symmetric product (7) generates an expansion based upon an average field within the aperture, not the total field produced by the aperture. By inspection, the real admittance is

$$\mathrm{Re}[Y_1 + Y_2]_h = \frac{Sk_2^2}{3\pi Z_2}. \tag{40}$$

The real (40) and imaginary (37) impedances only depend upon the material properties of region 2, while the combined impedances

in [5, Eq. (31)] depend upon both regions. In addition, the derived impedances differ from [5] by including the aperture area.

For the electric dipole admittance, divide (13) by b, substitute in (34) and (36) with $\mathbf{M} = V_e\hat{M}_e$ and solve for V_e. Using (21) and the input current (26), the imaginary admittance is

$$\mathrm{Im}[Y_1 + Y_2]_e = \frac{j\omega\epsilon_2 S b^2}{\alpha_e}. \tag{41}$$

Similarly, using the radiated power density of an electric dipole current near a conductor along with (13) and (36), the real admittance is

$$\mathrm{Re}[Y_1 + Y_2]_e = \frac{S b^2 k_2^4}{3\pi Z_2}. \tag{42}$$

Like the magnetic dipole impedance, these impedances only depend upon the material properties of a single region around the aperture, and differ from [5] by a factor Sb^2.

The aperture impedance for a given source is shared between both sides of the aperture. A parallel distribution is adopted in [5] though no justification is offered. Consider the dipole equivalent currents (34)–(35) for the individual half space aperture dipoles (28)–(31) in each region, where $\mu_2 \to \mu_1$ in (35) for region 1,

$$\mathbf{K}l_1 = -\mathbf{K}l_2 \tag{43}$$

$$\epsilon_1\mathbf{I}l_2 = -\epsilon_2\mathbf{I}l_1. \tag{44}$$

The magnetic dipole current (43) is the same on both sides of the aperture, implying a series distribution of impedance, while the distribution of electric dipole current (44) indicates a parallel distribution of impedance. While (43)–(44) are found in [5, Eqs. (27)–(28)], the equations are used to illustrate the relative magnitudes between the dipoles on both sides of the aperture, not to motivate an impedance distribution.

The magnetic dipole impedance is given by combining (37) and (40), inverting, then separating into two equal parts assuming a series distribution,

$$Z_{1h}^{\beta} = Z_{2h}^{\beta} = \frac{1}{2}\left(\frac{S k_2^2}{3\pi Z_2} + \frac{S}{j\omega\mu_2\alpha_{m\beta}}\right)^{-1}. \tag{45}$$

This impedance (45) is equivalent to a series combination of a resistor and inductor. When $\left(\frac{S}{\omega\mu_2\alpha_{m\beta}}\right)^2 >> \left(\frac{Sk_2^2}{3\pi Z_2}\right)^2$ or $k^6\alpha^2 << 1$, then the equivalent inductance and resistance may be written as

$$L = \frac{\mu_2\alpha_{m\beta}}{2S} \tag{46}$$

$$R = \frac{Z_2\alpha_{m\beta}^2 k_2^4}{6\pi S}. \tag{47}$$

These equivalent circuit parameters are extracted simply by calculating the real and imaginary parts of (45).

The electric dipole impedance assuming a parallel distribution is

$$Z_{1e} = Z_{2e} = 2\left(\frac{Sb^2k_2^4}{3\pi Z_2} + \frac{j\epsilon_2\omega Sb^2}{\alpha_e}\right)^{-1} \tag{48}$$

equivalent to a series combination of a resistor and capacitor, with extracted values of

$$C = \frac{\epsilon_2 Sb^2}{2\alpha_e} \tag{49}$$

$$R = \frac{2Z_2\alpha_e^2k_2^2}{3\pi Sb^2}. \tag{50}$$

when $k^6\alpha^2 << 1$. When wavelengths approach the size of the aperture, (45) and (48) must be used to generate the circuit impedance.

4. APERTURE CIRCUIT

While the aperture impedances in [5] are incorporated into a more generalized matrix method, here the impedances are combined together to form an effective circuit. Since both the electric and magnetic dipoles can be excited simultaneously, the effective impedances representing those aperture dipoles are combined in parallel. This combined impedance forms the basis of the analytical description of diffracted power through the aperture, calculated using the mismatch in the source wave impedance compared to the aperture impedance. This transmitted power is also limited by aperture boundary conditions that reduce field strengths in the aperture based upon the materials on each side. Power transmitted into the aperture circuit is radiated into both regions, divided based upon the behavior of image currents created around the aperture.

For a source in region 1, the aperture impedance along $n = \hat{\beta}, \hat{\gamma}$ is given by a parallel combination of magnetic and electric dipole impedances for region 2 (45), (48)

$$Z_a^n = Z_{2h}^n || Z_{2e} = \frac{Z_{2h}^n Z_{2e}}{Z_{2h}^n + Z_{2e}}. \tag{51}$$

Since the aperture impedance depends upon the region containing the source, a source in region 2 should be considered independently using dipole impedances for region 1.

The power in the incident magnetic field and available to the magnetic dipole is integrated over the aperture area to obtain the total

available power

$$P_{inc} = \frac{Z_1 S}{2} | < \mathbf{H}_{10}, \hat{M}_{hi} > |^2 \tag{52}$$

where $\mathbf{H}_{10}$ is the incident field. The mismatch in impedance between the source region and the aperture only allows a fraction of this total power into the aperture. Using the fractional power transmitted for a normally incident wave at the interface of two different impedances [26], Z_1 for region 1 and Z_a^n for the aperture, the reduction in power (52) is

$$P_{impd}^n = Re\left(\frac{4Z_1 Z_a^{n*}}{|Z_1 + Z_a^n|^2}\right) \tag{53}$$

where $*$ denotes the complex conjugate.

In addition, the materials on either side of the aperture reduce the magnitude of the magnetic field within the aperture, further reducing available power. This boundary condition on the magnetic field is present in the half space magnetic moment (29), but was removed (33) in the process of combining the two half space dipoles to determine the aperture impedance. Imposing this boundary condition expressed in terms of the incident magnetic field in (52) and including (53), the total power transmitted into the aperture and radiated is

$$P_{mag}^n = \frac{4\mu_1^2}{(\mu_1 + \mu_2)^2} \frac{Z_1 S}{2} | < \mathbf{H}_{10}, \hat{M}_{hi} > |^2 P_{impd}^n. \tag{54}$$

The equivalence of the parallel distribution of magnetic polarizability (19) to the electric polarizability reduces the power radiated by the aperture electric dipole. However, given the parallel combination of electric and magnetic dipole impedances, only the magnetic dipole impedance is observed below the aperture dipole resonance. To obtain an electric dipole power required by the square of (19)

$$P_e \propto \frac{\alpha_{m\gamma}^2 \alpha_{m\beta}^2}{(\alpha_{m\gamma} + \alpha_{m\beta})^2} \tag{55}$$

some combination of magnetic dipole powers must be used. Since the fractional power (53) is proportional to α_{mn}^2, to obtain (55) it is postulated that

$$P_{impd}^e = \frac{P_{impd}^\beta \alpha_{m\gamma}^2 \cos^2\theta + P_{impd}^\gamma \alpha_{m\beta}^2 \sin^2\theta}{(\alpha_{m\gamma} + \alpha_{m\beta})^2}. \tag{56}$$

The product $P_{impd}^\beta \alpha_{m\gamma}^2$ replicates the numerator in (55) and similarly when $\beta \to \gamma$, dividing the electric dipole power based upon the components of the incident magnetic field along $\hat{\beta}$ and $\hat{\gamma}$. This ensures

that the electric dipole displays the same resonance characteristics of the magnetic dipoles that are also excited by the incident wave. The total power in the incident electric field available to the electric dipole is

$$P_{inc} = \frac{S}{2Z_1} | < \mathbf{E}_{10}, \hat{M}_e > |^2. \tag{57}$$

Including the boundary conditions from the half space dipole moment in region 2, the total power radiated is

$$P_e = \frac{4\epsilon_2^2}{(\epsilon_1 + \epsilon_2)^2} \frac{S}{2Z_1} | < \mathbf{E}_{10}, \hat{M}_e > |^2 P^e_{impd}. \tag{58}$$

Not all of the power transmitted into the aperture radiates into region 2, some is radiated back into region 1. Previously [5], the back scattered dipole was treated in the same way as the forward scattered dipole field. Alternately, the back-scattered dipole is treated here as the result of image currents.

The forward scattered dipole induces image currents in the conductor surrounding the aperture to satisfy boundary conditions, eliminating the tangential electric field caused by the aperture dipole along the plane conductor. By continuity, these currents can not simply stop at the aperture edge nor can the currents enter the conductor replacing the aperture. Thus, it is presumed that the image currents in region 2 travel through the aperture into region 1. This naturally leads to an inverted orientation of region 1 currents compared to region 2, consistent with known behavior.

The image currents alone in region 1 produce an image dipole field. Without a corresponding 'real' dipole, this image field violates boundary conditions along the plane conductor. To satisfy the boundary conditions, the image field must itself create a dipole image in the aperture. An image of an image is real, thus creating a 'real' aperture dipole. Since the backscattered dipole only exists to support the presence of the image currents, the power in the region 1 dipole is the same as the power in the image field in region 1. Thus, the total power radiated by the aperture is

$$P_e + P_{mag} = P_{2ap} + P_2^{img} + 2P_1^{img} \tag{59}$$

where P_{2ap} is the power directly radiated by the aperture in region 2, P_2^{img} is the power in the image field in region 2 and $2P_1^{img}$ accounts for the image field and the 'real' dipole in region 1.

The power in the image fields is determined by using the total power radiated by a dipole near a conductor [23, Eqs. (3)–(11)],

$$P = g(k_i) P_{dipole} \tag{60}$$

$$P_{image} = (g(k_i) - 1) P_{dipole} \tag{61}$$

where P_{dipole} [23, Eqs. (2)–(116)] is the power radiated by an isolated dipole, P_{image} is the power in the image field and $g(k_i)$ is the relative increase in power due to the image currents,

$$g(k_i) = \left(1 - \frac{3\cos 2k_i h}{(2k_i h)^2} + \frac{3\sin 2k_i h}{(2k_i h)^3}\right) \tag{62}$$

where h is the effective distance of the aperture dipole from the plane conductor. Substituting the power directly radiated by the aperture into region 2 for P_{dipole}, the power in the image field is

$$P_2^{img} = (g(k_2) - 1)\, P_{2ap} \tag{63}$$

$$2P_1^{img} = 2\,(g(k_1) - 1)\, P_{2ap}. \tag{64}$$

Since the magnetic currents recreating the aperture have an associated length and the electric dipole is normal to the aperture, it will appear to the far field observer to be located away from the aperture. The minimum distance for a dipole of length l to adopt any orientation without intersecting the plane conductor is $h = l_e/2$. For a circular aperture, $h = 2a$.

Substituting (63)–(64) into (59) to solve for P_{2ap}, the total power radiated into region 2 is

$$P_2 = P_{2ap} + P_2^{img} = \frac{g(k_2)}{2g(k_1) + g(k_2) - 2}\left(P_{mag}^{\gamma} + P_{mag}^{\beta} + P_e\right) \tag{65}$$

while the power radiated into region 1 is

$$P_1 = 2P_1^{img} = \frac{2g(k_1) - 2}{2g(k_1) + g(k_2) - 2}\left(P_{mag}^{\gamma} + P_{mag}^{\beta} + P_e\right). \tag{66}$$

At low frequencies, $g(k) = 2$ and equal power is radiated into each region. At high frequencies $g(k) = 1$ and $P_1 = 0$, there is no backscattered field. In the transition from wavelengths much larger than the aperture to wavelengths comparable to the aperture, the leading factor in P_1 becomes negative, increasing the power radiated into the forward direction.

For long incident wavelengths, the source impedance is greater than the aperture impedance, $Z_1 >> Z_a^n$, and the power radiated by the aperture can be compared to previous dipole solutions. Consider the magnetic dipole power, (54). The fractional power (53) becomes $\mathrm{Re}(4Z_a^{n*}/Z_1)$ and the real part of the aperture impedance (45) reduces to

$$Z_a^n = \frac{64 Z_2 k_2^4 a^6}{54\pi S}. \tag{67}$$

Substituting the magnetic dipole power (54) into (65) and (66), equal power is radiated into each region. Consistent with previous results for

aperture dipole power [7, 13, 25], the power radiated by the magnetic dipole into region 2 is

$$P_{mag}^{n} = \frac{4\mu_1^2}{(\mu_1+\mu_2)^2}\frac{64Z_2k_2^4a^6}{54\pi}|H_{10}^{\tan}|^2 \tag{68}$$

and the electric dipole power is

$$P_e = \frac{4\epsilon_2^2}{(\epsilon_1+\epsilon_2)^2}\frac{64Z_2k_2^4a^6}{216\pi}\frac{|E_{10}^{nrm}|^2}{Z_1^2}. \tag{69}$$

For an obliquely incident wave, the same radiated power relations are expected. Given that fields in the aperture are the result of global currents in the plane conductor scattering from the aperture as indicated in [27], the power transmitted into the aperture is determined by the global currents incident upon the aperture impedance. Since the currents exciting the aperture are confined to the same plane regardless of the orientation of the incident plane wave, the relations obtained from normal incidence are expected to apply for oblique incidence.

5. NUMERICAL MODEL

To confirm the derived impedances, the behavior of an aperture in a plane conductor was investigated using ANSYS® Academic Research, v. 11.0, a commercial finite element method (FEM) software package. A square transverse electromagnetic (TEM) waveguide was used to direct an input wave towards a circular aperture in a perfect conductor, radiating into an approximate half space. The half space is constructed using perfectly matched layers (PML), a computational method that absorbs incident radiation but produces little reflection, approximating an infinite space.

The geometry is illustrated in Fig. 2. The aperture of radius a and thickness d utilizes a curved transition to the plane conductor in an effort to minimize gradients in the calculated field and maintain numerical accuracy. Due to symmetry of the fields and geometry, only one quarter of the system is modeled (not shown).

The TEM waveguide is constructed using perfect electric (PEC) and magnetic conductors (PMC) along the transverse boundaries as appropriate. The input wave is created using a matched impedance port, producing little reflection for waves reflected back towards the source.

The bulk of the input waveguide and radiation region was meshed using brick elements while the aperture used a tetrahedral element. A transition region utilized pyramid shaped elements to change smoothly from the tetrahedrals in the aperture to the bricks outside. The use

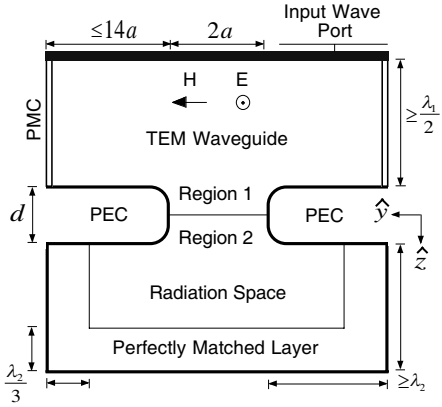

Figure 2. Numerical model geometry. Not to scale.

of pyramids limits all elements to first order; one component of the electric field per element edge, and one normal component per element face. There is a minimum of 4 elements along $\hat{z}$ through the aperture. Due to software restrictions, this could not be increased.

The power radiated by the aperture was calculated by summing the time averaged Poynting flux through elements in a planar slice cut through the middle of the aperture and parallel to the aperture plane. Similar values are obtained using ANSYS supplied functions for calculating power in the far field.

The impedance of the aperture was calculated using the field definitions of voltage and current

$$-\int_{l_1}^{l_2} \mathbf{E} \cdot d\hat{l} = V \tag{70}$$

$$\oint \mathbf{H} \cdot d\hat{l} = I \tag{71}$$

in the plane of the aperture and using $V/I = Z$. The paths for the electric and magnetic fields are along the incident fields through the aperture center. The closed loop for the magnetic field traverses both sides of the aperture. If the total field field is calculated using the FEM rather than the scattered field alone, the magnetic field is integrated along one side of the aperture and doubled due to symmetry.

6. RESULTS

Figure 3 compares the aperture circuit described in (Section 4) and the ANSYS average real and imaginary impedance for an aperture

excited by a normally incident plane wave source in region 1. For low frequencies, both the real and imaginary impedance of the aperture circuit correspond extremely well with the numerical model. A reduced real impedance is expected for the numerical model due to the decrease in radiated power from the aperture thickness [15]. The computed real and imaginary aperture impedance vary by less than 15% and 10% respectively over the whole aperture area (not shown), with less than 5% variation between $0 < \rho < 0.8a$. Thus, the average aperture impedance description presented here is appropriate.

The power radiated into region 2 from the aperture circuit model and ANSYS is compared in Fig. 3(c). The long dashed black line is the transmission coefficient as determined by Bouwkamp [14] which includes dipole, quadrupole, and octupole radiation. The circuit power matches the power radiated by the aperture dipoles in the low frequency limit, up to the peak in dipole impedance. As expected, at higher frequencies the dipole moment is not sufficient. Even though the total numerical impedance decreases after the dipole peak, the power continues to increase, particularly noticeable as the material indices for region 2 increase. This indicates that higher order aperture modes should be considered individually when calculating radiated power.

The aperture circuit resonances in Fig. 3(b) for various materials in region 2 occur near the numerically obtained resonances. Similar results are observed for additional material configurations not shown. The increasing difference between the dipole model and the numerical aperture starting below resonance is consistent with a series combination of impedance for higher order moments.

Figure 4 compares the Poynting flux in the aperture obtained with ANSYS to the predicted transmitted (54) and radiated (65), (66) power using the average ANSYS aperture impedance for Z_a. The power transmitted into the aperture (54) is double the Poynting flux into region 2 at low frequencies and similar at high frequencies. This dependence is consistent with the assumed power distribution using image theory where half of the power transmitted into the aperture goes into the forward scattered field at long wavelengths and all of the transmitted power is radiated through the aperture for short wavelengths. The difference between predictions and the Poynting flux at the peak in Fig. 4 is consistent with a need to treat the impedance of each mode separately, rather than the combined impedance illustrated.

The association of the region 1 dipole with an image field (66) leads to oscillations between radiating and absorbing power as the aperture transitions from low frequency dipole behavior to higher frequencies. The choice $h = 2.1a$ in (62) leads to a null in power for the region 1 dipole at the intersection between the predicted transmitted power

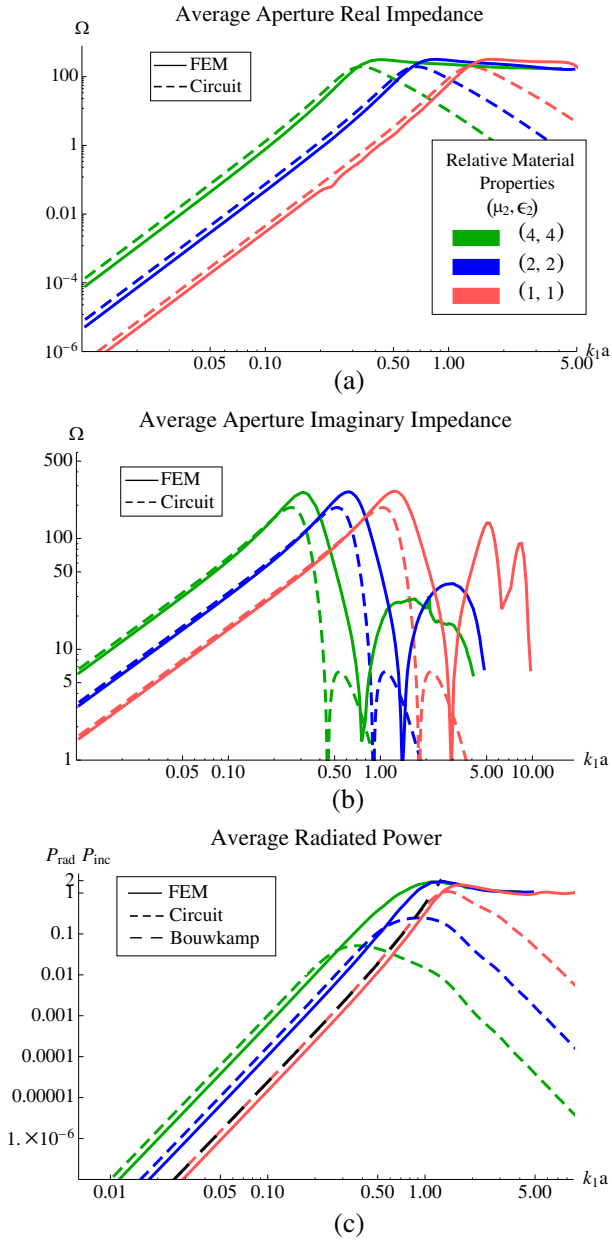

Figure 3. Magnitude of (a) real and (b) imaginary average impedance of aperture excited by normally incident wave using the presented aperture circuit and FEM; (c) power radiated into region 2. Numerics obtained with aperture radius to thickness ratio $a/d = 10$.

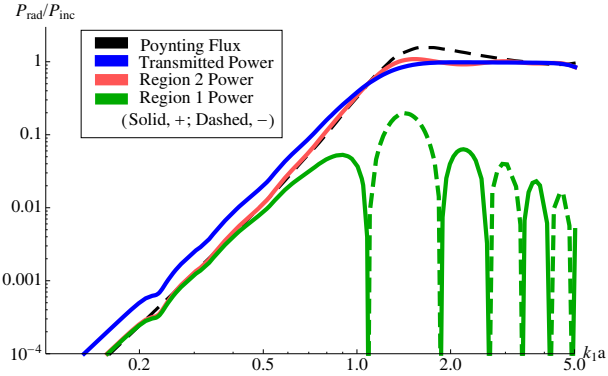

Figure 4. Distribution of power within the aperture for a normally incident plane wave with vacuum in both regions. The black line is the Poynting flux in the numerically modeled aperture. The blue line is the power transmitted into the aperture using (54), the red line is the power radiated into region 2 (65), and the green/brown line is the power radiated/absorbed in region 1 (66), all calculated using the average ANSYS aperture impedance and $h = 2.1a$.

and measured Poynting flux for vacuum near $k_1a \approx 1$. Thus, the proposed aperture model satisfies the conservation of power with the numerical model when using impedances obtained from the numerical model. The slight increase in h from predictions of $2a$ may be due to the thickness of the aperture $d = 0.1a$.

The accuracy of the numerical model has been estimated by comparison to a theoretical description of a circular aperture in a thick screen given by Roberts [16]. The method utilizes a sum of circular waveguide modes to describe power radiated by the aperture; the first fifteen modes were used to generate the solution for comparison with ANSYS (Fig. 5, black). In the low frequency regime, the error is less than 6%, reaching a maximum less than 20% as the aperture passes through resonance. The generally low percent error validates the ANSYS model.

The large percent error in radiated power between ANSYS and the aperture circuit is due to the reduction in power from the thickness of the aperture in ANSYS [15, 16]. However, the percent error for both power and real impedance are nearly the same, confirming the presented aperture real impedance. The percent error between ANSYS and the aperture circuit for the imaginary impedance is under 10% below $ka \approx 0.7$, at which point higher order moments become important. These results validate the aperture dipole circuit.

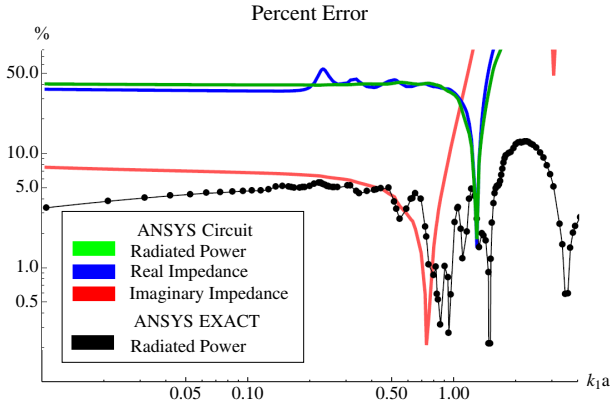

Figure 5. Percent error between the power radiated into region 2 in the FEM solution and a theoretical description of an aperture in a thick screen [16] excited by a normally incident plane wave (black). Percent error in real/imaginary (blue/red) impedance and power (green) between numerical model and presented aperture circuit for vacuum.

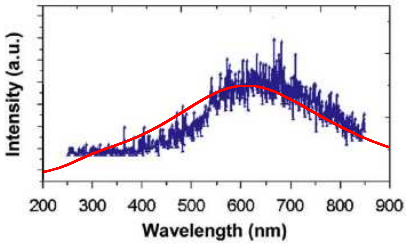

Figure 6. Radiated light (blue) for a circular aperture excited by a high energy electron beam measured by Degiron [17] compared to the predicted radiated power (65, red), using $a = 135$ nm, $h = 2.1a$.

The derived aperture circuit is compared to experimental results [17] of light radiated by a circular aperture ($a = 135\,\text{nm}$, $d = 200\,\text{nm}$) in a suspended Ag metal film excited by a high energy electron beam. An advantage of using a high energy electron source is there is no background signal from light not exciting the aperture dipole [17]. The power radiated by the aperture due to the input electron beam current is reproduced in Fig. 6 along with the predicted radiated power of the aperture. The measured peak in transmission is associated with a localized surface plasmon resonance and images of

the resonance confirm a dipole distribution [17]. The dipole aperture circuit yields a radiated power that closely matches the experimental results, up to a constant multiplicative factor due to the presentation of arbitrary units for the experimental results, supporting the presented radiated power derivation. The peak in radiated power using the presented aperture circuit is just under $1.1P_o$, where P_o is the incident power.

7. DISCUSSION AND CONCLUSION

The presented aperture circuit builds upon previous work [5] to derive new expressions for the dipole impedance of an aperture. The new impedances have been verified by comparison to a numerical investigation of a circular aperture using ANSYS. While ANSYS required significant computation times to determine the aperture impedance, using the presented dipole circuit yields the same impedance in seconds. The numerical model has been verified by comparison to previous numerical investigations [15] as well as an analytical description of an aperture using waveguide modes [16]. Further, the model presented for radiated power closely matches experimental observations of an aperture in a metal film excited by a high energy electron beam, supporting the derived expressions.

The presented aperture model also provides insight into low frequency diffraction. The derived aperture impedances are determined solely by the material properties of the region that does not contain the wave source. Further, power transmitted into the aperture is distributed into forward and backward scattered fields by image currents surrounding the aperture. This method also indicates that an aperture only produces a dipole for the forward scattered field. The backward scattered field is a product of image currents driven by the forward field. The derived impedances also demonstrate that apertures have a minimum effective thickness for electromagnetic diffraction. The same effective thickness is found for an aperture excited by an acoustic wave, radiating into a half space.

The derived aperture circuit offers a simple and effective method for describing the complex impedance and the power radiated by an aperture in a plane conductor for long wavelengths. In contrast to previous dipole solutions, the presented dipole circuit produces a radiated power that goes to zero in the high frequency limit. By converting Bethe's dipoles to an equivalent circuit, it is expected that a greater range of aperture problems may be solved without requiring numerical methods with significant computation times.

REFERENCES

1. Harrington, R. F., "Matrix methods for field problems," *Proceedings of the IEEE*, Vol. 55, No. 2, 136–149, 1967.
2. Harrington, R. F. and J. R. Mautz, "A generalized network formulation for aperture problems," *IEEE Transactions on Antennas and Propagation*, 870–873, 1976.
3. Harrington, R. F. and D. T. Auckland, "Electromagnetic transmission through narrow slots in thick conducting screens," *IEEE Transactions on Antennas and Propagation*, Vol. 28, No. 5, 616–622, 1980.
4. Harrington, R. F., "Resonant behavior of a small aperture backed by a conducting body," *IEEE Transactions on Antennas and Propagation* , Vol. 30, No. 2, 205–212, 1982.
5. Mautz, J. R. and R. F. Harrington, "An admittance solution for electromagnetic coupling through a small aperture," *Appl. Scien. Res.*, Vol. 40, 36–69, 1983.
6. Harrington, R. F. and J. R. Mautz, "Characteristic modes for aperture problems," *IEEE Transactions on Microwave Theory and Techniques*, Vol. 33, No. 6, 500–505, 1985.
7. Harrington, R. F. and J. R. Mautz, "Electromagnetic coupling through apertures by the generalized admittance approach," *Comput. Phys. Comm.*, Vol. 68, 19–42, 1991.
8. Wang, T., R. F. Harrington, and J. R. Mautz, "Electromagnetic scattering from and transmission through arbitrary apertures in conducting bodies," *IEEE Transactions on Antennas and Propagation*, Vol. 38, No. 11, 1805–1814, 1990.
9. Leviatan, L., R. F. Harrington, and J. R. Mautz, "Electromagnetic transmission through apertures in a cavity in a thick conductor," *IEEE Transactions on Antennas and Propagation*, Vol. 30, No. 6, 1153–1165, 1982.
10. Liang, C. and D. K. Cheng, "Generalized network representations for small-aperture coupling between dissimilar regions," *IEEE Transactions on Antennas and Propagation*, Vol. 31, No. 1, 177–182, 1983.
11. Hsi, S., R. F. Harrington, and J. R. Mautz, "Electromagnetic coupling to a conducting wire behind an aperture of arbitrary size and shape," *IEEE Transactions on Antennas and Propagation*, Vol. 33, No. 6, 581–587, 1985.
12. Jeng, S. K., "Scattering from a cavity-backed slit in a ground plane-TE case," *IEEE Transactions on Antennas and Propagation*, Vol. 38, 1523–1529, 1990.

13. Bethe, H., "Theory of diffraction by small holes," *Phys. Rev.*, Vol. 66, No. 7–8, 163–182, 1944.
14. Bouwkamp, C. J., "Diffraction theory," *Rep. on Prog. in Phys.*, Vol. 17, 35–100, 1954.
15. Garcia de Abajo, F. J., "Light transmission through a single cylindrical hole in a metallic film," *Opt. Exp.*, Vol. 10, No. 25, 1475–1484, 2002.
16. Roberts, A., "Electromagnetic theory of diffraction by a circular aperture in a thick, perfectly conducting screen," *J. Opt. Soc. Am.*, Vol. 4, No. 10, 1970–1983, 1987.
17. Degiron, A., H. J. Lezec, W. L. Barnes, and T. W. Ebbesen, "Optical transmission properties of a single subwavelength aperture in a real metal," *Opt. Comm.*, Vol. 239, No. 1–3, 61–66, 2004.
18. Rayleigh, L., *Theory of Sound*, Dover Publications, New York, 1945.
19. Blackstock, D. T. *Fundamentals of Physical Acoustics*, Wiley-Interscience, New York, 2000.
20. Chang, C., A. K. Sarychev and V. M Shalaev, "Light diffraction by a subwavelength circular aperture," *Laser Phys. Lett.*, Vol. 2, 351–355, 2005.
21. Ebbesen, T. W., H. J. Lezec, H. F. Ghaemi, T. Thio, and P. A. Wolff "Extraordinary optical transmission through sub-wavelength hole arrays," *Nature*, Vol. 391, 667–669, 1998.
22. Genet, C. and T. W. Ebbesen, "Light in tiny holes," *Nature*, Vol. 445, No. 7123, 39–46, 2007.
23. Harrington, R. F., *Time-Harmonic Electromagnetic Fields*, IEEE Press, 2004.
24. Gluckstern, R. L. and R. K. Cooper, "Electric polarizability and magnetic susceptibility of small holes in a thin screen," *IEEE Transactions on Microwave Theory and Techniques*, Vol. 38, No. 2, 186–192, 1990.
25. De Meulenaere, F. D. and J. Van Bladel, "Polarizability of some small apertures," *IEEE Transactions on Antennas and Propagation*, Vol. 25, No. 25, 198–205, 1977.
26. Jackson, J. D., *Classical Electrodynamics*, 3rd edition, John Wiley and Sons, New York, 1999.
27. Bortchagovsky, E., G. Colas Des Francs, D. Molenda, A. Naber, and U. C. Fisher, "Transmission of an obliquely incident beam of light though small apertures in a metal film," *Appl. Phys. B*, Vol. 85, No. 1–2, 49–53, 2006.